DOI: http://dx.doi.org/10.22104/ijhfc.2016.465

Iranian Journal of Hydrogen & Fuel Cell 3(2016) 167-182

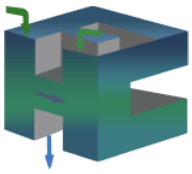

Iranian Journal of Hydrogen & Fuel Cell

IJHFC

Journal homepage://ijhfc.irost.ir

The effect of vertical injection of reactants to the membrane electrode assembly on the performance of a PEM fuel cell

Farzin Ramin[1], Sima Baheri Islami[1*], Siamak Hossainpour[2]

[1]**Faculty of Mechanical Engineering, University of Tabriz, Tabriz, Iran**
[2]**Faculty of Mechanical Engineering, Sahand University of Technology, Tabriz, Iran**

Article Information

Article History:

Received:
15 Sep 2016
Received in revised form:
18 Dec 2016
Accepted:
26 Dec 2016

Keywords

PEM fuel cell
Vertical injection
Numerical modeling
Polarization
MEA

Abstract

In order to present a new and high performance structure of PEM fuel cell and study the influence of the flow direction and distribution on the rate of reactants diffusion, three novel models of vertical reactant flow injection into the anode and cathode reaction area field have been introduced. They consist of one inlet, two inlets, and a continuous channel. The governing equations on the steady three dimensional non-isothermal flow have been discretized using the finite volume method. These 3D simulations evaluate the effectiveness of flow direction on the transportation and chemical phenomena inside the PEM fuel cell by applying the computational fluid dynamics (CFD) method to the transportation and conservation equations with the suppositions of steady state and one phase flow. The numerical results are validated with experimental ones for available common fuel cells. The results show that the presented geometries have several mechanical and chemical benefits, such as extra diffusion of reactants, because of flow direction, improvement of species distributions, enhancement in temperature management and more effective water removal due to the number of outlets and uniform current distribution. Furthermore, the continuous channel inlet presents a substantially higher performance than the others due to covering more reaction area and having a high rate of reactants diffusion. With regard to the polarization curve along with other advantages, the mentioned design can be strongly recommended to obtain high operating efficiency and can be considered for the manufacture of a new generation of PEM fuel cells in the form of high performance stacks.

[*]Corresponding Author's Fax: +984133354153
E-mail address: baheri@tabrizu.ac.ir

1.Introduction

A PEM fuel cell is an effective new device with a simple mechanism in which electrical energy with green emissions can be attained by the released energy of chemical reactions. Recently, most investigations of PEMs have been conducted on their cost of manufacturing, better performance, and durability which are the most challenging problems in promoting fuel cell technology. In order to achieve this, many researchers have concentrate mentioned problems [1-4]. Many researchers have tried to overcome the high cost, low performance and durability [5-8], yet enhancement of cell performance and manufacturing cost remain unsolved [9, 10].

There are many important parameters which have a major effect on fuel cell performance. Some challenges facing PEMs are the conditions of the operational system, the chemical and mechanical properties of the component of fuel cells, and the improvement of the gas distribution over the MEA by means of gas channels geometry. In addition, an efficient structure along with approaching and supplying reactants appropriately to obtain a uniform current density inside the cell play crucial roles in the performance, durability and cost of PEMFC [11-12]. Some review, such as the high mass of the brittle graphite bipolar plates that yield to high values of weight and large occupied volume, the uneven distribution and low diffusion of reactants into the catalyst layer, the out of standard working range of temperature and the low amount of outlet current density and performance, needs to be done in terms of technical, mechanical and economic problems on conventional models of PEMFCs.

Some research has been done to improve performance by using different configurations of flow fields, such as interconnected single and double serpentine design, design. Some researches have been done on the geometries of flow channel and study in this field continues. [13, 14]. Yu and Su [15] investigated some conventional structures such as serpentine and parallel geometry designs. They found that the cell with a serpentine gas channel had a higher performance than the ones with parallel geometry. Lorenzini-Gutierrez et al. [16] studied a new geometry called the tree shaped channel with a radial structure. This research was done to decrease the pressure loss by enlarging the reaction area to improve the efficiency. Results show that the novel introduced structure is the best choice among the other geometric designs due to less pressure loss. Sierra et al. [17] proposed a newer design of a mixture of conventional and tubular configurations. They concluded that the conventional tubular geometry was the best choice due to the decrease in pressure drop and efficient water removal from the cell which led to an increment of the reactants concentration in the gas diffusion layer. One of the most necessary factors for improving the performance is to expand the reaction active area.

Pourmahmoud et al. [18] enhanced the conventional geometry of the cell by applying a deflection to the membrane electrode assembly which led to an increment in the flow velocity in the channel and in the excessive penetration of species to the reaction area. Nowadays researchers are concentrating on the geometry of fuel cells because applying a new design has the potential to produce the greatest effect among all other parameters to enhance the cell performance. Some researchers have investigated spiral geometries but this structure has some drawbacks like difficulty in manufacturing. In this regard, Escobar et al. [19] presented a spiral geometry that produced an even current density distribution and less pressure drop. Juarez et al. [20] investigated the benefits of a concentric spiral geometry on the performance of fuel cell stacks. Cano et al. [21, 22] recently presented a radial flow. The study was implemented to investigate the influence of a radial gas field on the velocity and the effect of flow inlet number on cell performance. The simulations showed that the low velocity at the end of the gas fields caused poor efficiency.

As mentioned above, one of the parameters that has a great deal of effect on performance and direct association with performance is the reactants channel structure embedded in the stack. In this

regard, Torkavannejad et al. [23] introduced novel geometries called circular, square and octagonal duct-shaped architectures to increase the outlet current density and reduce the cost and weight. Furthermore, they changed the MEA arrangement in which every MEA is in connection with two cathodes and vice versa. With this arrangement, not only did the outlet performance increase remarkably, but also the bipolar, which is the main and heaviest part, decreased about 40%. Wang et al. [24] improved a modification by embedding a baffle in the serpentine configuration allowing high performance to be achieved in PEMFCs at high current density. Additionally, in their study some dimensions were optimized. Dimensions, such as channel height, yielded better reactant transport to reaction area. Alvarado et al. [25] introduced a symmetric flow pattern which obtained higher performance due to an efficient channel structure for spreading the reactants. Chen et al. [26] studied novel flow field modification such as z-type and interdigited channels.

Measuring heat transfer coefficients for the millions of small holes inside the micro-structural gas diffusion layer is very difficult, experimentally or numerically. Sadeghifar [27] presented analytical models to predict the coefficient of heat transfer for both through-plane and in-plane flows inside fibrous media such as gas diffusion layers. Porosity and pore size data have long been used for reconstructing (two directional) fibrous materials. Sadeghifar [28] revealed a technical method for reaching fiber spacing from pore size (diameter) data. In this regard, the presented research indicated that the traditional concept, in which fibrous materials with lower porosity have higher thermal conductivity, did not necessary hold. Sadeghifar et al. [29] also revealed the results of a study on polymer electrolyte membrane fuel cells and found that "the thermal contact resistance increases with porosity'' isn't always true.

Recently some studies have focused on enlarging and developing the reaction area to obtain a high rate of chemical reaction along the channel [30-31]. Tiss et al. [32] studied numerically and experimentally partially blocked channels and their effects on performance and reactant transportation. They also investigated the optimized angle of inclination. The attained results showed that increasing the degree tilt up to 4.9 led to better performance, but increasing this value more had an extremely opposite effect. Walckzy et al. [33] provided uniform current density and more economical cells by using ribbon MEA architectures. In another study, Tseng et al. [34] proposed to use metal foam as a flow distributor in order to reduce the weight and volume of the PEM fuel cell. Their investigations showed that a PEM fuel cell with this novel characteristic as flow distributor presented some unique results compared with the conventional PEM unit cell with a traditional flow field plate as flow distributor. Less mass transport limitation and lightweight plus better electrical conductivity were the main advantages of the introduced distributor plates. Bilgili et al. [35] performed simulations in which an obstacle was used in the flow field at different boundary and inlet conditions. They concluded that by adding an obstacle in the channel flow field, reactants diffusion and distribution could be improved by a significant amount through the gas diffusion layer (GDL) which leads to performance improvement. Inset Vazifeshenas et al. [36] introduced and investigated the effect of appropriate compound flow on performance and water flooding. Their numerical simulation showed that there was an actual direct linkage between performance and channel design, and flooding can be prevented by using well-designed patterns. In this regard, their research showed that the compound design worked as well as the serpentine design and in some terms surpassed it, remarkably. Khazaae et al. [37] presented a unique annular and duct-shaped model for PEMFCs with novel patterns that could begin a new generation of fuel cells, solve some of the technical issue, and remarkably enhance the performance.

According to these explanations, designing appropriate structures provides a range of technical and economic benefits, and this will only be achieved

by moving from the conventional fuel cell to a new version of the structure. In this study, three channel designs composed of one and two vertical reactants inlets and the continuous channel inlet are presented. This type of PEM fuel cell configuration enhances the reactants diffusion and leads to an increase of the reaction rate. These architectures have the same boundary conditions as the conventional PEM fuel cells and any feed compositions, relative humidity and flow rates can be considered for both anode and cathode. In the present research, a three-dimensional, one phase, non-isothermal model is considered for this novel direct injection PEM fuel cell. Through computational fluid dynamics analysis and by comparing the polarization curves, this present study investigates the advantages of these three novel architectures over the conventional PEM fuel cells and the benefits that they can provide in terms of the uniformity of the temperature, current and reactant distributions inside the stack, and the cost and size reduction of PEM fuel cells.

2. Materials and Methods

2.1 Geometry and operational parameters

Fig. 1 indicates the schematic of both the new model with vertical injection of reactants and the conventional base model. The vertical injection is done by three new inlet configurations which are shown in Fig. 2. It consists of one inlet, two inlets, and a continuous channel inlet to investigate the effect of vertical injection geometry on the cell performance. Due to the low speed of reactants, the heights of bipolar plates and flow channels have been reduced to improve the efficiency of vertical injection. The outlets are at the both ends of the anode and cathode channels. Table 1 summaries the geometrical parameters and operation conditions [23]. The cell consists of hydrogen and oxygen channels, bipolar plates on the cathode and anode side of the cell which act as current collector with high electronic conductivity, and the membrane electrode assembly (MEA) located between gas channels. These fuel cells have the same active and operation condition as the base model. This allows comparison of these three PEM fuel cell configurations in the same conditions. This configuration leads to the introduction of a new type of cells, especially in terms of the way reactants are supplied, less volume occupied due to smaller bipolar plates, and the potential for enhancing the PEM fuel cell performance.

2.2 Assumptions

The main assumptions of this study are listed below:

- Ideal gas mixtures are assumed.
- Steady state condition and non-isothermal design are considered.
- The fully humidified inlet reactant condition for both anode and cathode is used.
- Negligible Ohmic resistance is considered at porous

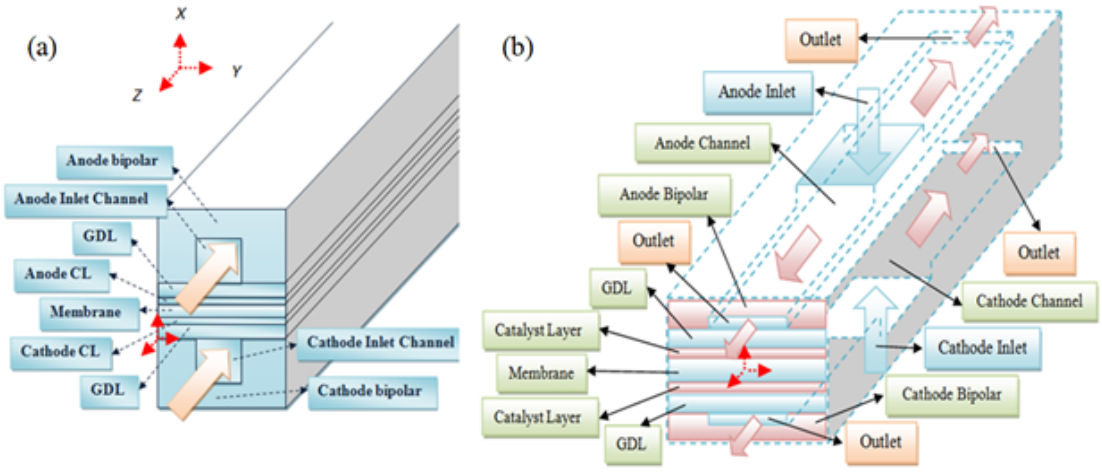

Fig. 1. The schematics of a) base model and b) the new vertical injection model.

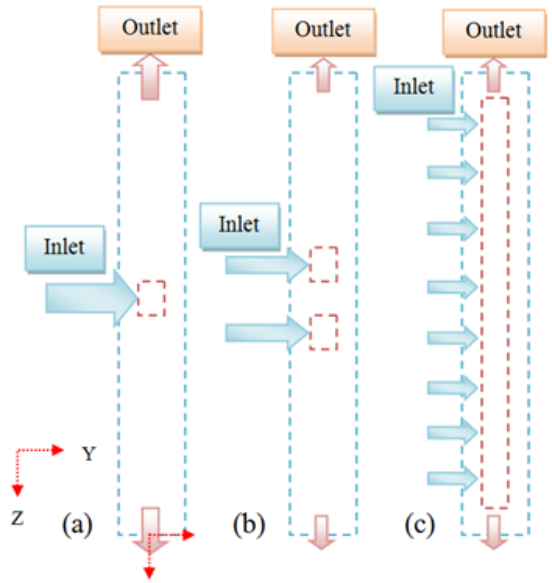

Fig. 2. A top view of the three proposed vertical injection models with a) one inlet, b) two inlets, and c) a continuous channel inlet.

electrodes and current collectors.

• Gas diffusion and catalyst layers are homogeneous and isotropic porous mediums.

• The flow is incompressible and laminar due to the low pressure gradients and flow velocities.

• The membrane is impermeable to cross-over of reactant gases and assumed to be fully humidified to transport the protons.

• The reactants diffusion obeys the dilute solution theory.

• The model is called a single phase simulation because of the liquid phase water produced during the reactions is not sensible and phase changes are not considered.

Table. 1. Geometrical and Operational Parameters

parameters	Symbol	Value	Unit
Channel length	L	0.05	m
Channel width	W	1 e^{-3}	m
Channel height	H	0.1 e^{-3}	m
Inlet length	L_{inlet}	1 e^{-3}	m
Inlet width	W_{inlet}	1 e^{-3}	m
Inlet channel length	$L_{inlet\ ch}$	3 e^{-2}	m
Shoulder area width	W_s	0.5 e^{-3}	m
Gas diffusion layer thickness	d_{GDL}	0.26 e^{-3}	m
Wet membrane thickness (Nafion 117)	$\hat{o}_{mem}$	0.23 e^{-3}	m
Catalyst layer thickness	$\hat{o}_{CL}$	0.0287 e^{-3}	m
Anode/Cathode catalyst layer porosity	ε	0.4	-
Anode/Cathode gas diffusion layer porosity	ε	0.4	-
Anode pressure	P_a	3	atm
Cathode pressure	P_c	3	atm
Inlet fuel and air temperature	T_{cell}	353.15	K
Thermal conductivity	k	0.15	W/K.m
Relative humidity of inlet fuel and air (fully humidified conditions)	Ψ	100	%
Reference current density	I	10	A/cm^2
Inlet anode oxygen mass fraction	$Y_{OXYGEN,A}$	0	-
Inlet anode hydrogen mass fraction	$Y_{HYDROGEN,A}$	0.3780066	-
Inlet anode water mass fraction	$Y_{WATER,A}$	0.6219934	-
Inlet cathode water mass fraction	$Y_{WATER,C}$	0.1031307	-
Inlet cathode oxygen mass fraction	$Y_{OXYGEN,C}$	0.2088548	-
Inlet cathode hydrogen mass fraction	$Y_{HYDROGEN,C}$	0	-

2.3. Governing equations

2.3.1. Gas flow fields

The governing equations on the reactants flow field for both anode and cathode sides [23] are the Continuity equation:

$$\nabla.\left(\rho u\right)=0 \tag{1}$$

and the Momentum conservation equation:

$$\nabla.\left(\rho uu\right)=-\nabla P+\nabla.\left(\mu\nabla u\right)-\frac{\mu}{K}\left(\varepsilon u\right) \tag{2}$$

The divergence of the mass flux through diffusion and convection present the mass balance of each species. The following equation presents the mass transport of species i [23]:

$$\nabla.[-\rho y_i\sum_{j=1}^{N}D_{ij}\frac{M}{M_J}\left(\nabla y_i+y_i\frac{\nabla M}{M}\right)+\rho y_i u]=0 \tag{3}$$

In which the subscript i presents oxygen at the cathode side, and hydrogen at the anode side; also the subscript j describes water vapor in both sides. Nitrogen is the third species at the cathode side. j ranges from 1 up to N where N=2 (for anode) and N=3 (for cathode).

The experimental terms based on the kinetic gas theory leads to Maxwell-Stefan diffusion coefficients for two different species which are dependent on temperature and pressure [23].

$$D_{ij}=\frac{T^{1.75}\times10^{-3}}{P\left[\left(\sum_k V_{ki}\right)^{\frac{1}{3}}+\left(\sum_k V_{kj}\right)^{\frac{1}{3}}\right]^2}\left[\frac{1}{M_i}+\frac{1}{M_j}\right]^{1/2} \tag{4}$$

In the above equation, the unit of pressure is in [bar], and the binary diffusion coefficient is in [cm^2/s]. The values for $\sum Vk_i$ are given by Fuller et al. [39], and the convective energy equation will yield the temperature fields;

$$\nabla.\left(\rho C_p uT-k\nabla T\right)=0 \tag{5}$$

2.3.2. Gas diffusion layers

Transport in a porous media is the pattern for the simulation of the gas diffusion layer. The following equations describe continuity, momentum and mass transport of species, respectively [23]:

$$\nabla.\left(\rho\varepsilon u\right)=0 \tag{6}$$

$$u=\frac{Kp}{\mu}\nabla P \tag{7}$$

$$\nabla.\ [-\rho\varepsilon y_i\sum_{j=1}^{N}D_{ij}\frac{M}{M_j}\left(\nabla y_i+y_i\frac{\nabla M}{M}\right)+\rho\varepsilon y_i u]=0 \tag{8}$$

The Bruggemann equation is used to correct the diffusion coefficients due to geometric constraints of the porous media [23]:

$$D_{ij}^{eff}=D_{ij}\times\varepsilon^{1.5} \tag{9}$$

The next equation describes the heat transfer process [23]:

$$\nabla.(\rho\varepsilon CpuT-k_{eff}\varepsilon\nabla T)=\varepsilon\beta\left(T_{solid}-T\right) \tag{10}$$

In which, the terms on the right-hand side denotes the heat transfer to or from the solid matrix of the gas diffusion layer. Here, β is a modified heat transfer coefficient that denotes the convective heat transfer in [W/m^2] and the specific surface area [m^2/m^3] of the porous media. So, the measurement unit of β is [W/m^3]. The potential distribution in the GDL is governed by the following equation:

$$\nabla.\left(\sigma_e\nabla\varnothing\right)=0 \tag{11}$$

In which, $\sigma_e=\sigma_0\exp[-B/(T-T_0)]$ is the membrane ionic conductivity $(ohm.m)^{-1}$ of the cell where σ_0 $(ohm.m)^{-1}$, B (K), and T_0 (K) are constants. In this model, the electron transport and ion transport are considered; therefore, the potentials of the solid

phase and the membrane phase are not constant. The membrane phase potential is calculated in the membrane and the catalyst layer and the solid phase potential is calculated in the gas diffusion and catalyst layer.

2.3.3. Catalyst layers

The thin layer of catalyst between the membrane and gas diffusion layers is where the sink and source terms of conservation equations are involved. This so called layer considers the sink term at the cathode side for oxygen as [23]:

$$S_o = -\text{——} i_c \quad (12)$$

Whereas, the sink term of the anode side for the hydrogen species is implemented as:

$$S_{H_2} = -\frac{M_{H_2}}{4F} i_a \quad (13)$$

The following equation simulates the produced water during the electrochemical reaction:

$$S_{H_2O} = -\frac{M_{H_2O}}{2F} i_c \quad (14)$$

The heat generation in the cathode catalyst layer is due to the entropy alteration and also irreversibility during the reaction [23]:

$$q = [\frac{T(-\Delta s)}{n_e F} + \eta_{act,c}] i_c \quad (15)$$

The Butler-Volmer equation simulates the distribution of current density as well as the relation of overpotential and exchange current density [23]:

$$i = i_O^{ref} \left[\exp\left(\frac{\alpha_a zF}{RT} \eta_{act} \right) - \exp(-\frac{\alpha_c zF}{RT} \eta_{act} \right) \quad (16)$$

Where the activation potential is defined as:

$$\eta_{act} = E - E_{eq} \quad (17)$$

Activation polarization loss is a specified ratio of energy needed to activate the electrochemical reaction. This phenomenon leads to a non-linear voltage drop which is called activation polarization. These losses occur in both anode and cathode catalyst layers.

2.3.4. Membrane

Water management at the membrane layer is due to the equilibrium of the water transfer from the anode to cathode side by electro osmotic drag as well as reverse transfer from the cathode to anode side via back diffusion. The net water flux presents the so called balance [23]:

$$N_W = n_d M_{H_2O} \frac{i}{F} - \nabla(\rho D_W \nabla y_w) \quad (18)$$

Where the subsequent equation presents the electro-osmotic drag coefficient:

$$n_d = \frac{2.5\lambda}{22} \quad (19)$$

In which, λ is the membrane water content. The heat transfer in the membrane will be presented by the next relation:

$$\nabla.(k_{mem} \nabla T) = 0 \quad (20)$$

Resistance to proton transport across the membrane is called potential loss and is governed by:

$$\nabla.(\sigma_e \nabla \varnothing) = 0 \quad (21)$$

2.4. Boundary conditions

Constant mass flow rate at the channel inlet, constant pressure condition at the channel outlets, and no mass flux conditions at all of the walls and symmetrical condition at the side faces are applied. All three inlet configurations have the same mass flow rates. For the momentum conservation equation, fuel velocity is specified at each inlet of anode and cathode flow channel. The velocity is calculated based on the concept of stoichiometry, which means “the required

amount of fuel at a given condition" [23]. The inlet mass fractions are determined by the inlet pressure and humidity according to the ideal gas law. The equations for both inlets are expressed as [23].

$$\left|\vec{u}\right|_{in} = \frac{\zeta}{X_{H_{2,in}}} \frac{i_{avg}}{2F} \frac{RT_{in}}{P_{in}} \frac{A_{MEA}}{A_{ch}} \quad (22)$$

In which, i_{avg} is the average current density at a given cell-potential. R, T_{in}, P_{in}, and ζ are the universal gas constant, inlet temperature, inlet pressure and the stoichiometric ratio, respectively. The stoichiometric ratio is defined as the ratio between the amount of supplied and the amount of required reactant on the basis of the reference current density i_{avg}, accordingly.

2.5. Numerical method

The governing equations were solved using finite volume software FLUENT. The SIMPLE algorithm (Fig. 3) was used for pressure-velocity coupling. The convergence criterion was less than 10^{-7} for all variables and average computational time for solving the set of equations was about six hours.

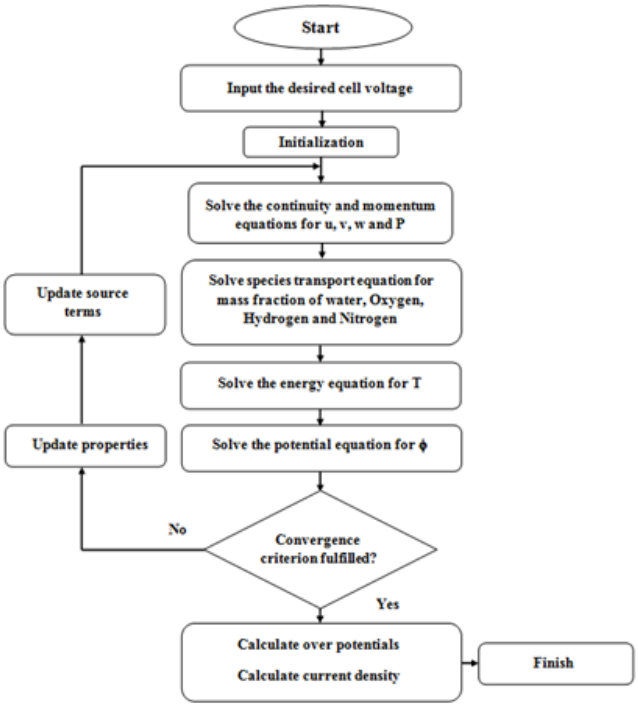

Fig. 3. The SIMPLE algorithm.

3. Results and discussions

In order to validate the numerical results, the polarization curve for the base model is compared with experimental results of Al-Baghdadi et al. [38] in Fig. 4. It shows good agreement between the results. It is worth noting that there is not good agreement in the high current density zone. This fact is the result of neglecting liquid water. The water formed in the catalyst layer is in the vapor phase in the numerical simulation. In fact, liquid water fills the pores of the catalyst and gas diffusion layers and does not let the oxygen molecules transfer to the catalyst layer easily leading to the loss of species.

One example of the grid independency test can also be seen in Fig. 4. It is obvious that 176,000 cells is a good choice from both accuracy and computational time aspects.

The comparison of the performance of the new PEM fuel cells proposed in this study with the conventional cell is performed through polarization curves as shown in Fig. 5. It is observed that all of the new configurations have higher performance than the base model; and at medium to high current density, which is the typical operating condition of PEM fuel cells, the proposed architectures significantly improve the performance in comparison with the conventional configuration. Also, the cell performance increases with the uniformity of vertical injection. So, the geometry with continuous vertical injection produces more current density than the other ones.

Three planes have used for indicating the distribution of various parameters in the subsequent sections and are shown in Fig. 6.

One of the most important factors in the chemical reaction is the species of hydrogen, its mass fraction distribution is represented in Fig. 7. As observed in flow fields, the concentration of hydrogen decreases gradually from inlet to outlet of the channel due to consumption and reaction of hydrogen at the catalyst layer. Results indicate that the mass fraction

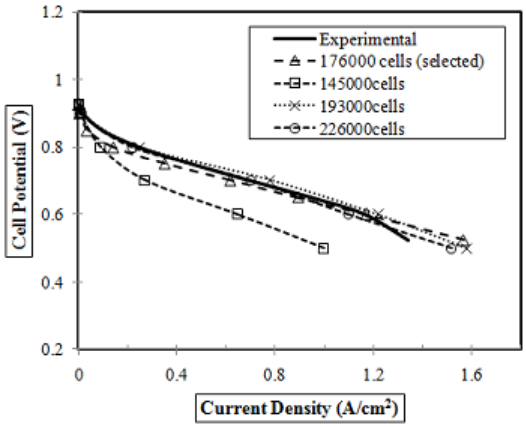

Fig. 4. Comparison of base model numerical results with experimental results of Al-Baghdadi et al. [38].

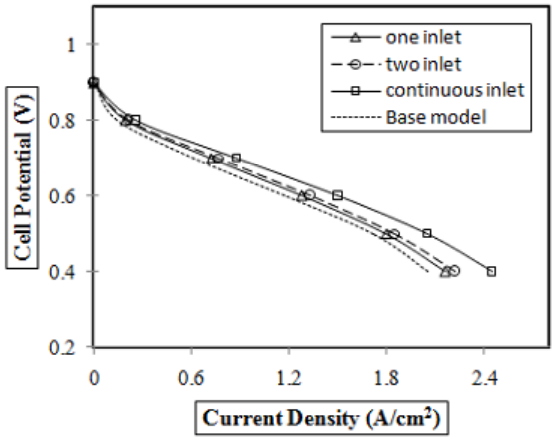

Fig. 5. Variation of cell performance with a) one inlet, b) two inlets, and c) a continuous inlet.

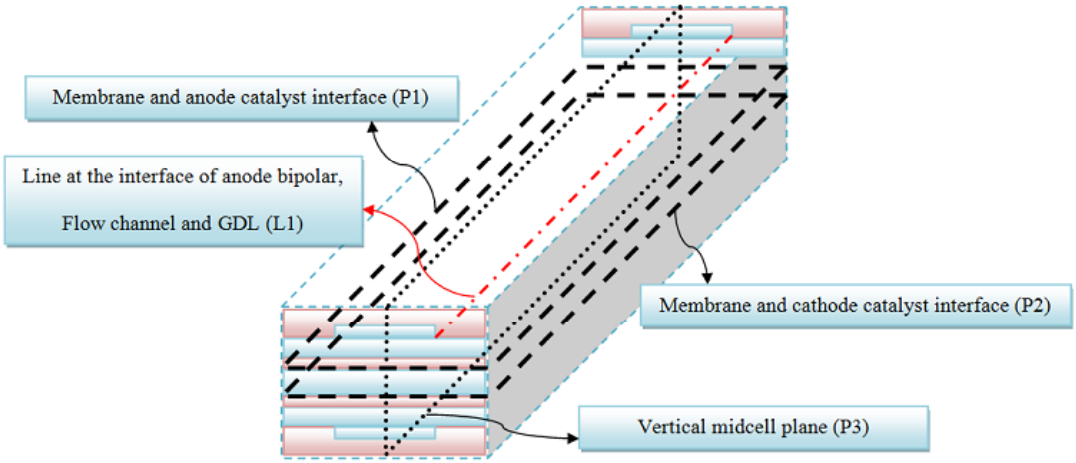

Fig. 6. Three planes used for indicating the results.

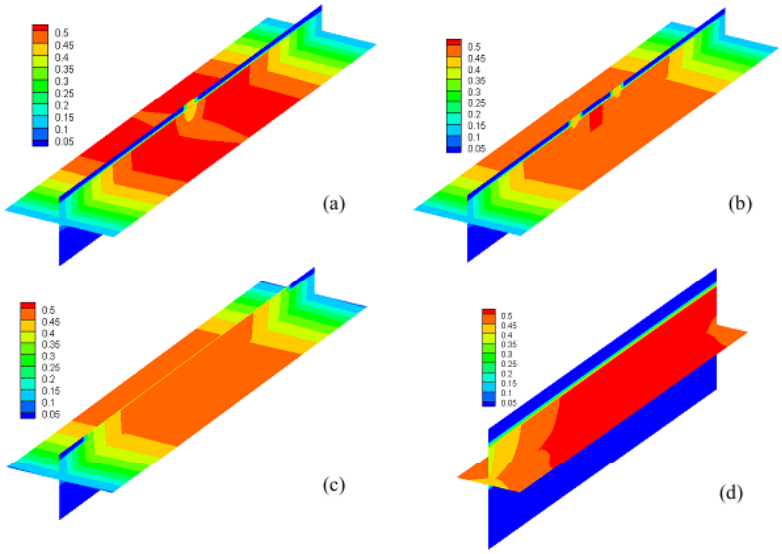

Fig. 7. Hydrogen mass fraction distribution along the P1 and P3 at V = 0.6 V with a) one inlet, b) two inlets, c) continuous channel inlet, and d) base model.

of the hydrogen decreases as the vertical injection area increases. All three novel geometries present distribution which, in comparison with the base model, do not suffer from the lack of enough penetration of anode side reactant. As it is clear, the case with continuous channel inlet indicates more consumption of hydrogen which could be attributed to the vertical injection of species.

Fig. 8 shows the distribution of oxygen mass fraction along the intersection of the cathode catalyst and membrane layers, which decreases along the channel to the outlets due to the consumption of specieswithin the catalyst layer. Oxygen as the cathode side reactant plays a critical role in the performance of the cell. The main purpose of the designed models is enhancement of species diffusion and was reached in these simulations to varying degrees. The figure indicates that the species concentrations have a direct relation with the inlet area of injection. With regard to this issue, the continuous channel inlet is preferred due to a uniform profile for the oxygen concentration and also more consumption which will lead to more current density in the cell.

The water vapor mass faction in both the vertical mid-cell plane and membrane-anode catalyst interface is indicated in Fig. 9 at 0.6 V. The water production due to the oxygen consumption, due to the electrochemical reaction at the cathode catalyst layer and the net water transfer through the membrane by the proton ions from anode to cathode side, are the main reasons for the water mass fraction increase and decrease along the cathode and anode sides, respectively. However, the magnitude of water mass fraction is higher and lower at the cathode and anode sides, respectively, as the inlet mouths increase to the continuous channel inlet mouth case, due to more available reactant gases in the diffusion bed for higher rate of electrochemical reaction.

Fig. 10 shows the temperature distribution along the cell at 0.6 V for the base model and the three new cases. It is obvious that the highest temperature occurs at the cathode catalyst layer due to the exothermic electrochemical reaction in this layer. The figure indicates that the temperature distribution is decreasing along the cell toward the outlets due to (1) the formation of water vapor which absorbs the produced heat for condensation and (2) the contact surface with bipolar plates which leads to heat conduction in the shoulder zones. It is clear that the maximum temperature region occurring in the cell,

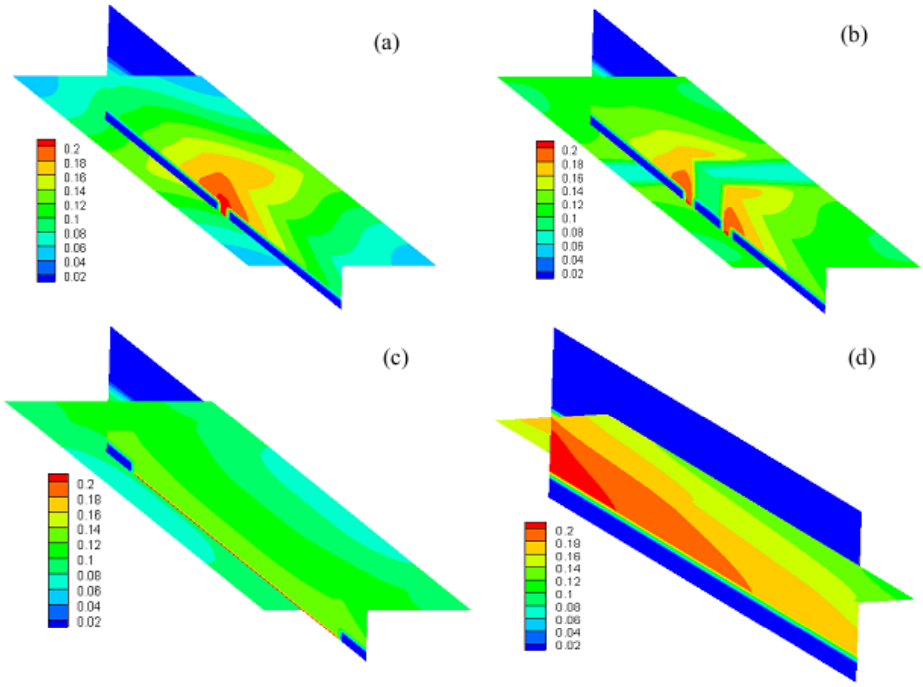

Fig. 8. Oxygen mass fraction distribution along the P2 and P3 at V = 0.6 V with a) one inlet, b) two inlets, c) continuous channel inlet, and d) base model.

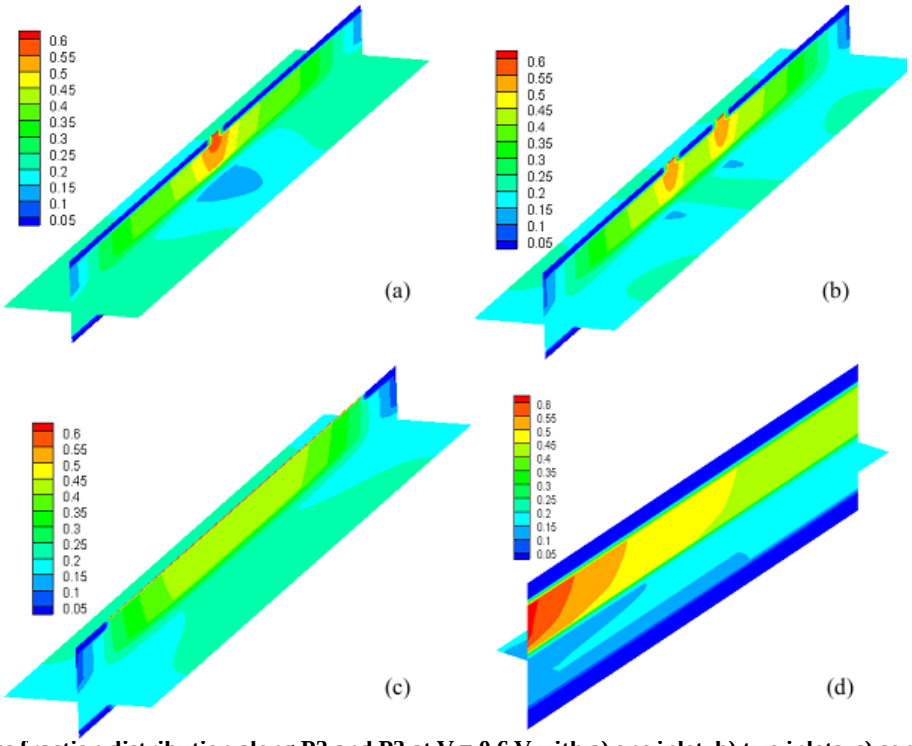

Fig. 9. Water vapor mass fraction distribution along P2 and P3 at V = 0.6 V with a) one inlet, b) two inlets, c) continuous channel inlet, and d) base model.

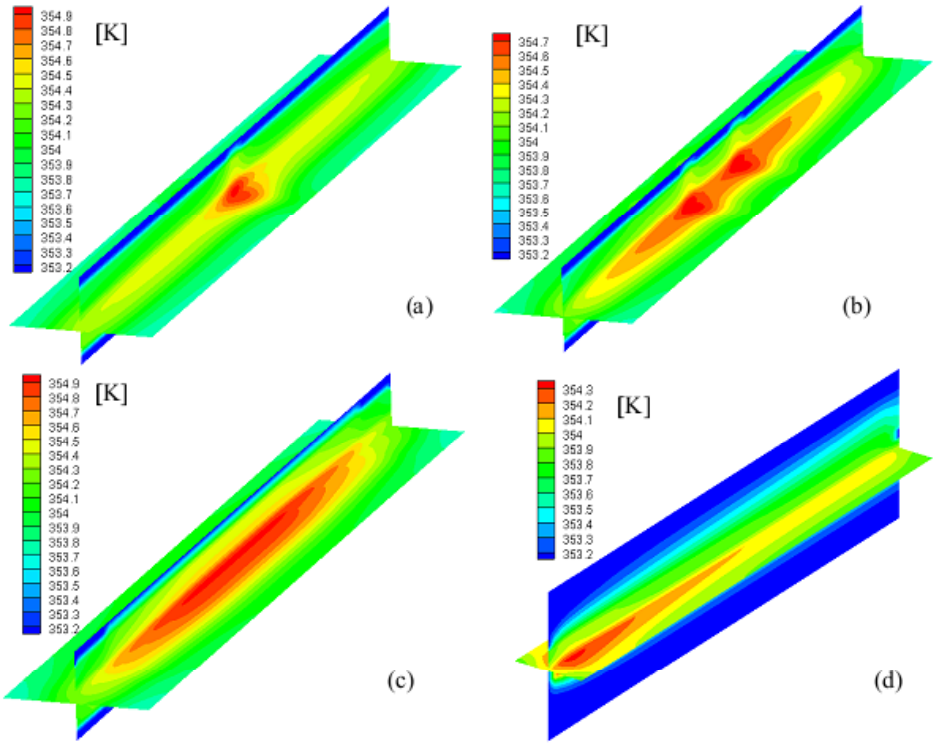

Fig. 10. Temperature distribution along the P2 and P3 at V = 0.6 V with a) one inlet, b) two inlets, c) continuous channel inlet, and

increases by increasing the number of inlets due to the decrease of the overpass distance of gases on the surface, which decreases their temperature . Also, Fig. 10 indicates that for continuous channel inlet (case c); the temperature gradient along the cell is more uniform compared with other cases due to the uniform diffusion of reactants for the electrochemical reaction. The current density distribution along the cell is shown in Fig. 11 at 0.6 V. Maximum magnitude of current density is related to the joint surfaces of the gas diffusion layer and the bipolar plates due to thepassing of electrons to the external circuit. Fig. 11 indicates

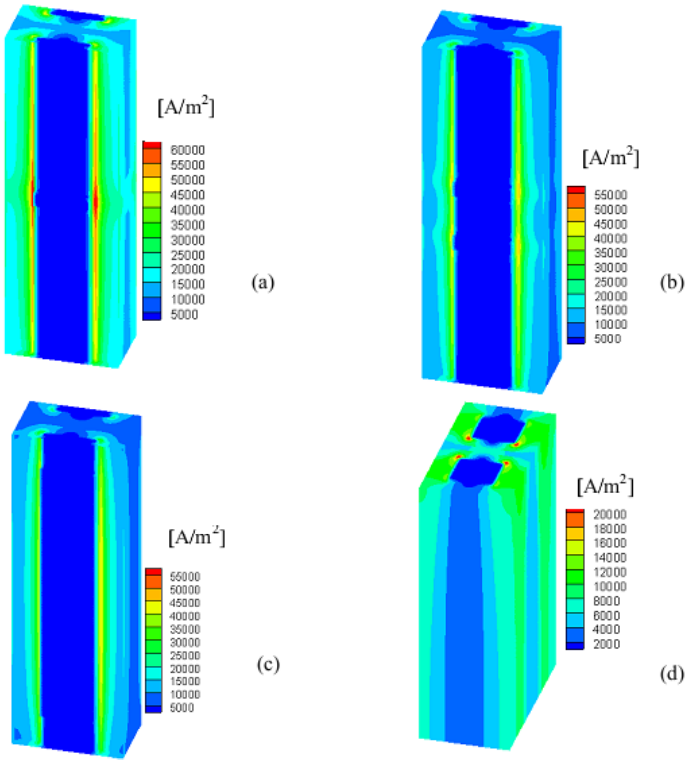

Fig. 11. Current density distribution along the cell at V = 0.6 V with a) one inlet, b) two inlets, c) continuous channel inlet, and d) base model.

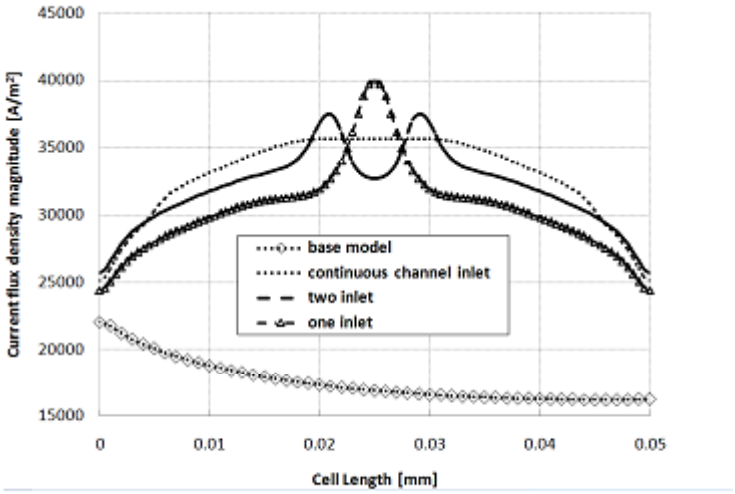

Fig. 12. Current density distribution along line (L1) at V = 0.6 V with a) one inlet, b) two inlets, c) continuous channel inlet, and d) base model.

that the maximum current density increases in the new models and also the increasing extent of inlets. Fig. 12 shows the current density distribution along the line (L1) which has been introduced in Fig. 6 at the interface of anode GDL, flow channel and bipolar plate for the base and three new models. It is obvious that the current density distribution is more uniform in the case with continuous channel inlet due to the uniform distribution of reactants which leads to improved efficiency.

4. Conclusions

A complete three dimensional, non-isothermal and single phase computational fluid dynamic model for a PEM fuel cell was used to investigate the effect of vertical injection of reactants to the gas diffusion layer on the performance, gas concentration, current density and temperature distribution. The conservation equations for different layers were solved numerically using the finite volume method which led to an acceptable agreement between the model and experimental data for a wide range of current densities. The following results were found:

1. The cell performance increased as the inlet mouths increase up to the continuous channel case due to the uniform diffusion of reactants.
2. When the inlet mouth of reactants changed to a continuous channel inlet, the hydrogen and oxygen consumption and also water production increased. Also, this channel mouth inlet case yielded a more uniform distribution of species.
3. A long temperature counter peak in case three indicates a maximum electrochemical reaction rate which leads to more current density.
4. The maximum local current density occurred at the inlet area and the interfaces of gas diffusion layer and bipolar plates, and the magnitude of current density decreased along the channel as a result of fewer amounts of species.
5. Up to 30% less occupied volume as compared to the conventional (base) configuration of a single cell of PEMFCs.
6. Although the new design presented in this manuscript improves the overall performance of PEM fuel cells, it would be very costly and difficult for practical stack implementation, but with the increasing development of production methods as well as with regard to efficiency and high performance yield, manufacturing the new geometry soon will be affordable.

Nomenclature

a	Water activity
A	Area (m^2)
C	Molar concentration (mol/m^3)
D	Mass diffusion coefficient (m^2/s)
E	Electrode potential (V)
E_{eq}	Equilibrium potebtial (V)
F	Faraday constant (C/mol)
I	Local current density (A/m^2)
i_o	Exchange current density (A/m^2)
k	Thermal conductivity (W/K.m)
K	Permeability (m^2)
M	Molecular weight (kg/mol)
n_d	Electro-osmotic drag coefficient
P	Pressure (Pa)
R	Universal gas constant (J/mol.K)
S	Entropy (J/K)
T	Temperature (K)
t	Thickness (m)
u	Vector of velocity (m/s)
V	Cell voltage (V)
V_{oc}	Open-circuit voltage (V)
W	Width (m)
X	Mole fraction
Y	Mass fraction
z	Number of electrons involved in electrode reaction

Greek Letters

α	Charge transfer coefficient, (dimensionless)
μ	Viscosity (kg/m.s)
ζ	Stoichiometric ratio
λ	Water content of membrane
σ_e	Membrane ionic conductivity (1/ohm.m)
ε	Porosity

η Over potential (V)
ρ Density (kg/m^3)
ϕ Potential (V)

Subscripts and Superscripts

a Anode
avg average
c Cathode
ch Channel
cl Catalyst
eff Effective
GDl Gas diffusion layer
k Chemical species
m Membrane
MEA Membrane electrolyte assembly
ref Reference value
sat Saturated
w water

References

[1] Kim Y.S., Kim .SI., Lee N.W., Kim M.S., "Study on a purge method using pressure reduction for effective water removal in polymer electrolyte membrane fuel cells", Int. J. Hydrogen Energy, 2015, 40: 9473.

[2] Taspinara R., Litster S., Kumbur E.C., "A computational study to investigate the effects of the bipolar plate and gas diffusion layer interface in polymer electrolyte fuel cells", Int. J. Hydrogen Energy, 2015, 40: 7124.

[3] Verma A., Pitchumani R., "Influence of transient operating parameters on the mechanical behavior of fuel cells", Int. J. Hydrogen Energy, 2015, 40: 8442.

[4] Jeon Y., Na H., Hwang H., Park J., Hwang H., Shul Y., "Accelerated life-time test protocols for polymer electrolyte membrane fuel cells operated at high temperature", Int. J . Hydrogen Energy, 2015, 40: 3057.

[5] Sadeghifar H., Djilali N., Bahrami M., "Effect of polytetrafluoroethylene (PTFE) and micro porous layer (MPL) on thermal conductivity of fuel cell gas diffusion layers: modeling and experiments", J. Power Sources, 2014, 248: 632.

[6] Sadeghifar H., Bahrami M., Djilali N., "A statistically based thermal conductivity model for PEMFC gas diffusion layers", J. Power Sources, 2013, 233: 369.

[7] Sadeghifar H., Djilali N., Bahrami M., "A new model for thermal contact resistance between fuel cell gas diffusion layers and bipolar plates", J. Power Sources, 2014, 266: 51.

[8] Sadeghifar H., Djilali N., Bahrami M., "Thermal conductivity of a graphite bipolar plate (BPP) and its thermal contact resistance with fuel cell gas diffusion layers: effect of compression, PTFE, micro porous layer (MPL), BPP out-of flatness and cyclic load", J. Power Sources, 2015, 273: 96.

[9] Mert S.O., Ozcelik Z., Dincer I., "Comparative assessment and optimization of fuel cells", Int. J. Hydrogen Energy, 2015, 40: 7835.

[10] Wei Z.h., Su K., Sui S.H., He A., Du S.H., "High performance polymer electrolyte membrane fuel cells (PEMFCs) with gradient Pt nanowire cathodes prepared by decal transfer method", Int. J. Hydrogen Energy, 2015, 40: 3068.

[11] Limjeerajarus N., Charoen-amornkitt P., "Effect of different flow field designs and number of channels on performance of a small PEFC", Int. J. Hydrogen Energy, 2015, 40: 7144.

[12] Arvay A., French J., Wang J.C., Peng X.H., Kannan AM., "Nature inspired flow field designs for proton exchange membrane fuel cell", Int. J. Hydrogen Energy, 2013, 38: 3717.

[13] Hsieh S.S., Yang S.H., Kuo J.K., Huang C.F., Tsai HH., "Study of operational parameters on the performance of micro PEMFCs with different flow fields", Energy Convers Manage, 2006, 47: 1868.

[14] Torkavannejad A., pesteei M., Khalilian M., Ramin F., Mirzaee I., "Effect of Deflected Membrane

Electrode Assembly on Species Distribution in PEMFC", International J. Eng. Transactions, 2015, 28: 3.

[15] Yuh M.F., Su A., "A three-dimensional full-cell CFD model used to investigate the effects of different flow channel designs on PEMFC performance", Int. J. Hydrogen Energy, 2007, 32: 4466e76.

[16] Lorenzini-Gutierrez D., Hernandez-Guerrero A., Ramos-Alvarado B., Perez-Raya I., Alatorre-Ordaz A., "Performance analysis of a proton exchange membrane fuel cell using tree-shaped designs for flow distribution", Int. J. Hydrogen Energy, 2013, 38:14750.

[17] Sierra J, Figueroa-Ramı´rez S.J, Dı´az S.E, Vargas J, Sebastian P.J., "Numerical evaluation of PEM fuel cell with conventional flow fields adapted to tubular plates", Int. J . Hydrogen Energy, 2014, 39(29):16694.

[18] Pourmahmoud N., Rezazadeh S., Mirzaee I., MotalebFaed S., "A computational study of a three-dimensional proton exchange membrane fuel cell (PEMFC) with conventional and deflected membrane electrode", J. Mech Sci. Technol, 2012, 26: 2959e68.

[19] Escobar-Vargas J.A., Hernandez-Guerrero A., Alatorre Ordaz A., Damian-Ascencio C.E., Elizalde-Blancas F., "Performance of a non-conventional flow field in a PEMFC", The 20th International Conference on Efficiency, Cost, Optimization Simulation and Environmental Impact of Energy Systems , Padova, Italy, 2007.

[20] Juarez-Robles D., Hernandez-Guerrero A., Ramos-Alvarado B., Elizalde-Blancas F., Damian-Ascencio C.E., "Multiple concentric spirals for the flow field of a proton exchange membrane fuel cell", J. Power Sources, 2011, 196: 8019e30.

[21] Cano-Andrade S., Hernandez-Guerrero A., Von-Spakovsky M.R., Rubio-Arana C., "Effect of the radial plate flow field distribution on current density in a proton exchange membrane (PEM) fuel cell", ASME International Mechanical Engineering Congress and Exposition, Seattle-Washington, United States of America, 2007.

[22] Cano-Andrade S., Hernandez-Guerrero A., Von Spakovsky M.R., Damian-Ascencio C.E., Rubio-Arana J.C., "Current density and polarization curves for radial flow field patterns applied to PEMFCs (proton exchange membrane fuel cells)", Energy, 2010, 35:920e7.

[23] Torkavannejad A., Sadeghifar H., Pourmahmoud N., Ramin F., "Novel architectures of polymer electrolyte membrane fuel cells: Efficiency enhancement and cost reduction", Int. J. Hydrogen Energy, 2015, 40:12466.

[24] Wang X.D., Huang Y.X., Cheng C.H., Jang J.Y., Lee D.J., Yan W.M., et al., "An inverse geometry design problem for optimization of single serpentine flow field of PEM fuel cell", Int. J. Hydrogen Energy, 2010, 35:4247.

[25] Ramos-Alvarado B., Hernandez-Guerrero A., Juarez-Robles D., Li L., "Numerical investigation of the performance of symmetric flow distributors as flow channels for PEM fuel cells international", Int. J. Hydrogen Energy, 2012, 37:436.

[26] Chen Y.S., Peng H., "Predicting current density distribution of proton exchange membrane fuel cells with different flow field designs", J. Power Sources, 2011, 196:1992.

[27] Sadeghifar. H., "In-plane and through-plane local and average Nusselt numbers in fibrous porous materials with different fiber layer temperatures: Gas diffusion layers for fuel cells", J. Power Sources, 2016, 325: 311.

[28] Sadeghifar H., "Reconstruction and analysis of fuel cell gas diffusion layers using fiber spacing rather than pore size data: Questioned validity of widely-used porosity-based thermal conductivity models", J. Power Sources, 2016, 307:673.

[29] Sadeghifara H., Djilalic N., Majid Bahramib M., "Counter-intuitive reduction of thermal contact resistance with porosity: A case study of polymer electrolyte membrane fuel cells", Int. J. Hydrogen Energy, 2016, 41:

6833.

[30] Friess B.R., Hoorfar M., "Development of a novel radial cathode flow field for PEMFC", Int. J. Hydrogen Energy, 2012, 37:7719.

[31] Surajudeen Olanrewaju O., "Performance enhancement in proton exchange membrane fuel cell-numerical modeling and optimization [PhD thesis]", University of Pretoria, 2012.

[32] Tiss F., Chouikh R., Guizani A., "A numerical investigation of reactants transport in a PEM fuel cell with partially blocked gas channel", Energy Conversion Management 2014, 80: 32.

[33] Walczyk D.F., Sangra J.S., "A feasibility study of Ribbon architecture for PEM fuel cells", ASME J. Fuel Cell Sci Technol, 2010, 7: 051001.

[34] Tseng C., Tsang Tsai B., Liu Z.H., Cheng T., Chang W., Lo S.H., "A PEM fuel cell with metal foam as flow distributor", Energy Conversion and Management, 2012, 62:14.

[35] Bilgili M., Bosomoiu M., Tsotridis G., "Gas flow field with obstacles for PEM fuel cells at different operating conditions", Int. J. Hydrogen Energy, 2016, 40:2303.

[36] Vazifeshenas Y., Sedighi K., Shakeri M., "Numerical investigation of a novel compound flow field for PEMFC performance improvement", Int. J. Hydrogen Energy, 2015, 40(16):15032.

[37] Khazaee I., Ghazikhani M., "Three-dimensional modeling and development of the new geometry PEM fuel cell", Arabian J. Sci. Eng., 2013, 38: 1551.

[38] Sadiq Al-Baghdadi Maher A.R., Shahad Al-Janabi Haroun A.K., "Parametric and optimization study of a PEM fuel cell performance using three-dimensional computational fluid dynamics model", Renew Energy, 2007, 32:1077.

[39] Fuller E.N., Schettler P.D., Giddings J.C., "New method for prediction of binary gas-phase diffusion coefficients", Int. Eng. Chem., 1966, 58:1.